Hindawi
International Journal of Aerospace Engineering
Volume 2018, Article ID 9247429, 9 pages
https://doi.org/10.1155/2018/9247429

Research Article

Development of a Novel Launch System Microwave Rocket Powered by Millimeter-Wave Discharge

Kimiya Komurasaki and Kuniyoshi Tabata

Department of Aeronautics and Astronautics, The University of Tokyo, 7-3-1, Hongo, Bunkyo, Tokyo 113-8656, Japan

Correspondence should be addressed to Kuniyoshi Tabata; k.tabata@al.t.u-tokyo.ac.jp

Received 22 January 2018; Revised 29 August 2018; Accepted 10 September 2018; Published 30 December 2018

Academic Editor: Angel Velazquez

This paper presents the state of art of *Microwave Rocket* development and related researches on atmospheric discharge in a high-power millimeter-wave beam. Its operational mechanisms, thruster design, history of development, and flight path and cost analyses are introduced along with millimeter-wave discharge observations and numerical simulations. A thruster model of 126 g weight with no on-board propellant was launched to 1.2 m altitude using a 1 MW class gyrotron. A flight analysis that shows 77% cost reduction is possible using *Microwave Rocket* as the first stage of H-IIB heavy. A millimeter-wave discharge with unique plasma structure such as a quarter-wavelength microstructure and a comb-shaped filamentary structure was observed and reproduced by a two-dimensional numerical model.

1. Introduction

Many recent studies have been devoted to wireless power transfer systems for flying objects using electromagnetic-wave radiation such as lasers and microwaves [1–3]. The use of electric power presents many benefits because of its efficiency, nontoxicity, and nonexplosive features. Beamed energy propulsion [4–15] used as a space transportation system gains its propulsive energy wirelessly from outside of the vehicle using beamed energy. Various propulsion mechanisms have been proposed as alternatives to conventional chemical rocket propulsion.

Space launch systems are powered by an electromagnetic-wave beam irradiating them from the ground, as depicted in Figure 1. In 2000, Myrabo demonstrated the launch of a thruster model using a 10 kW class pulsed CO_2 laser up to an altitude of 71 m in a flight lasting 12.7 s [9]. The vehicle, *Lightcraft*, weighed about 50 g and was driven by a laser-supported detonation (LSD). Parkin and Murakami proposed a microwave thermal thruster; the concept of which is to accelerate on-board propellant heated through a heat exchanger irradiated by a millimeter-wave beam from the ground [10]. The hydrogen propellant reaches double the exhaust velocity of LOX/LH2 rocket propellant.

In detonation-type thrusters, a laser or millimeter-wave induces atmospheric discharge. An ionization front propagates at a supersonic speed toward the energy source accompanying a shock wave. Such waves are designated as LSD or millimeter-wave-supported detonation (MSD), by which electromagnetic wave energy is converted directly and efficiently to thrust.

As described in this paper, a thruster driven by an atmospheric millimeter-wave discharge, *Microwave Rocket*, is introduced. *Microwave Rocket* is characterized by three features. First, it can achieve a high payload ratio because the vehicle need not load fuel and oxidizer on-board. Instead, it uses atmospheric air as a propellant during flight in a dense atmosphere. Second, once an electromagnetic-wave generator facility, such as gyrotrons, is built on the ground, it is reusable in multiple launches. Third, high-pressure gas for thrusting is produced through a millimeter-wave-supported detonation. Therefore, no turbo-pump system is required. For those reasons, *Microwave Rocket* is expected to achieve drastic launch cost reduction.

Figure 1: Artist image of beamed energy propulsion launcher.

A gyrotron is a high-power millimeter-wave oscillator that uses a cyclotron resonance maser phenomenon for energy conversion from electrical energy. The original purpose of the gyrotron development is heating plasma for nuclear fusion using electron cyclotron heating and current drive. In Japan at the National Institute for Quantum and radiological Science and Technology (QST, formerly the Japan Atomic Energy Agency), a gyrotron oscillating at 170 GHz has been developed for the International Thermonuclear Experimental Reactor (ITER) project [16–18]. The improvement of oscillation efficiency using the collection of depressed electrical energy enabled the output power of greater than 1 MW. Detailed characteristics of the QST gyrotron for the ITER project are presented in Table 1. A millimeter-wave beam is inferior to a laser beam in directivity, but millimeter-waves are attractive because the cost of gyrotron manufacture is lower than the laser oscillator cost by 2–4 orders of magnitude.

2. Thruster Structure and Engine Cycle

Microwave Rocket comprises a cylindrical tube in which an MSD wave propagates and a closed end, called a thrust wall, where high-pressure conditions are sustained. For air-breathing, reed valves are installed on the tube wall. Its engine cycle is identical to a typical pulse detonation engine cycle, as presented in Figure 2. (1) A millimeter-wave beam is line-focused by a conical concentrator. Atmospheric breakdown occurs near the thrust wall. (2) An MSD wave propagates toward the thruster exit, absorbing the incident millimeter-wave power. (3) At the time when the MSD wave is exhausted through the tube exit, the incident millimeter-wave pulse is suspended. At the same time, an expansion wave begins to propagate upstream in the tube from the exit to the thrust wall. (4) When the expansion wave reaches the thrust wall, it is reflected on the wall, generating negative gauge pressure inside the tube. Because of this negative pressure, reed valves open. Fresh air is taken passively. Impulsive thrust is generated intermittently by repeating this cycle.

A chemical detonation is settled down to a steady-state called a Chapman–Jouguet (C–J) detonation, which gives the highest pressure increase for a certain heat input [19]. On the other hand, the propagation velocity of a MSD wave is known to exceed the C–J velocity, as we call over-driven detonation. In order to predict the condition behind a blast wave, it is of much importance to examine the relationship between beam intensity and propagation velocity.

Table 1: Characteristics of QST gyrotron [16].

Frequency (wavelength)	170 GHz (1.77 mm)
Output power	>1 MW
Output duration	1 ms to 3600 s
Beam transverse mode	Gaussian
Electric efficiency	>50%

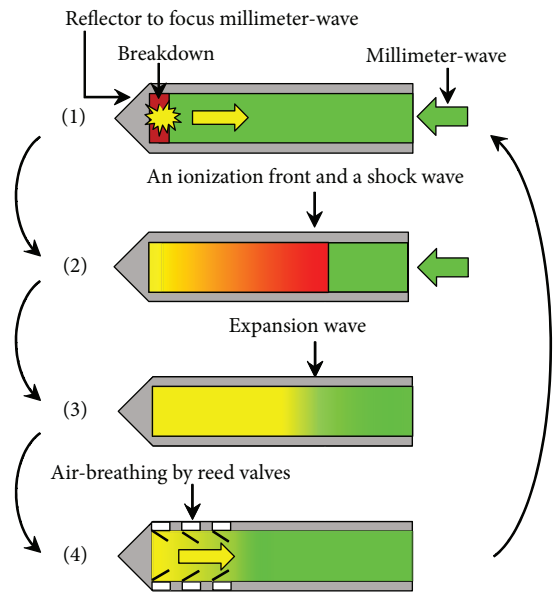

Figure 2: Pulse detonation engine cycle in *Microwave Rocket*.

3. Thruster Development and Launch Demonstrations

In 2001, plasma was ignited by focusing a beam launched from the QST gyrotron using a parabolic reflector under atmospheric conditions. In 2003, the first launch experiment used a 930 kW millimeter-wave beam in a single pulse operation. A miniature rocket model weighing 10 g was lifted to 2 m altitude (Figure 3) [20]. In the experiment, the maximum momentum coupling coefficient of 395 N/MW, defined as a ratio of total obtained impulsive thrust impulse to input energy, was achieved. This coefficient was comparable to that of a laser detonation thruster achieved using a solid-state laser with 2.0 J pulse energy in 2013 [21].

After optimizing operational parameters in a repetitive pulse mode and after developing a beam expander, a 126 g thruster model was launched to 1.2 m altitude in 2009 (Figure 4) [22]. Continuous generation of impulsive thrust was confirmed. In the repetitive pulse mode, impulses after the first impulse were found to decrease with residual air density inside the thruster tube, where air density decreases because of heating. However, experiments using a forced air-breathing system with a pressurized air tank proved that the impulse could be recovered with air refreshment inside the tube during the pulse interval [22].

In 2011, thrust was augmented by increases in output power of the gyrotron and in the thrust duty cycle, defined

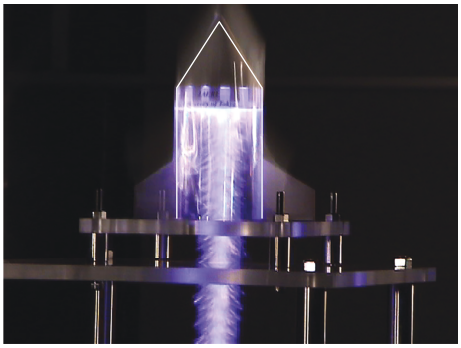

Figure 3: Launch demonstration with a 10 g thruster model conducted in 2003 [20]. Millimeter-wave discharge was photographed through a transparent thruster tube.

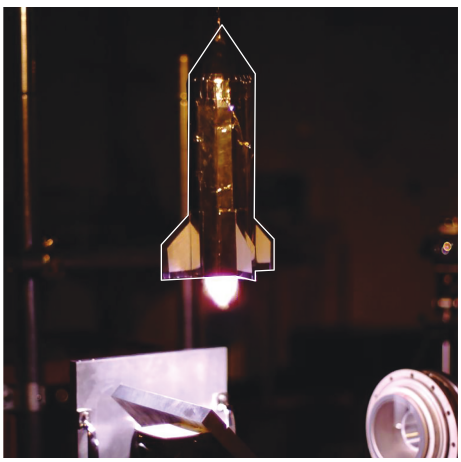

Figure 4: Launch demonstration with a 126 g thruster model in a multipulse operation in 2009 [22].

as a product of millimeter-wave pulse duration and pulse repetition frequency, as presented in Table 2 [23]. This experiment was made possible by the QST gyrotron, which had a high-voltage IGBT switch with switching speed that was higher than earlier versions. Because the achieved time-averaged thrust was as high as 30 N, a MW-class gyrotron can launch a kg-class vehicle. Therefore, a 1 kg thruster model launch is planned as the next step.

Reed valves with an inlet plenum are under development for efficient air-breathing during subsonic and supersonic flights at high altitudes. Reed valves open passively by the pressure difference between those inside and outside of the tube. A tapered-shape reed valve, which is capable of opening widely toward the inside without a stopper, was designed and tested [24]. A stopper designed to prevent plastic deformation of the valve was not used because it interacts with intense electromagnetic waves inside the tube. Air-breathing performance is evaluated by the partial filling rate (PFR) as represented by

$$\mathrm{PFR} = \frac{\text{Refreshed air volume}}{\text{Thruster tube volume}}. \quad (1)$$

Table 2: Thrust performance and operation conditions [23].

Year	2009	2011
Beam power @pulse repetition frequency	270 kW @ 50 Hz	570 kW @ 200 Hz
C_m	100 N/MW	360 N/MW
Time averaged thrust	2.3 N	30 N

According to a CFD analysis [25], a 10–15-fold thrust augmentation is expected using reed valves on the ground. At an altitude of 10 km and a flight Mach number of 2.0, the inlet plenum stagnates the flow and the thruster breathes the compressed air. The amount of compressed air to be breathed increases with the inlet plenum diameter, improving its air-breathing performance. The optimum inlet plenum diameter is determined by the balance between aerodynamic drag and air-breathing performance [26].

The altitude to which a vehicle continues to accelerate is theoretically proportional to the square of beam diameter: an approximately 40 cm beam diameter is necessary to achieve 10 m altitude; 6 m of beam diameter is necessary to achieve 100 km altitude. The beam intensity inside the tube is adjustable to achieve optimum detonation speed using a beam concentrator [27]. In 2012, a launch experiment with long beam transmission was conducted using a beam expander and concentrator. A ϕ 240 mm millimeter-wave beam was led into a thruster as shown in Figure 5, and the momentum coupling coefficient of 204 N/MW was obtained in a single-pulse operation, which was half as high as that in the short beam transmission experiment in 2003 [20]. In a multipulse operation, abnormal air breakdown was observed after the second pulse at the outlet of the thruster, resulting in a decrease of thrust force [28]. Because this phenomenon is considered due to the electrons remaining in the thruster, the pulse repetitive frequency is limited so that the pulse interval is long enough for the remaining electrons to be exhausted out of the thruster.

4. Feasibility Studies and Launch Cost Estimation

4.1. Replacement of H-IIB Launch Vehicle's First Stage by Microwave Rocket. Feasibility studies of transportation to low earth orbit and launch cost analyses for the *Microwave Rocket* have been conducted through subsonic to supersonic flight analyses. Fukunari et al. showed that the launch cost of the H-IIB heavy, which is capable of orbiting 19-ton payload to LEO, will be reduced by 77% by replacing its first stage including four SRBs by *Microwave Rocket*. The vehicle is significantly accelerated in a dense atmosphere and cut off at an altitude of 20.7 km with a velocity of 2 km/s. Using the conventional second stage, the payload ratio is enhanced to 0.155 which is 4.5 times as high as the one by the H-IIB heavy. The manufacturing cost as the first stage is estimated to be around 3 M$ and is considerably lower than the conventional H-IIB first stage which costs about 85 M$. For this flight, about 94,000 gyrotrons are necessary to generate 188 GW output power. The construction cost of gyrotron

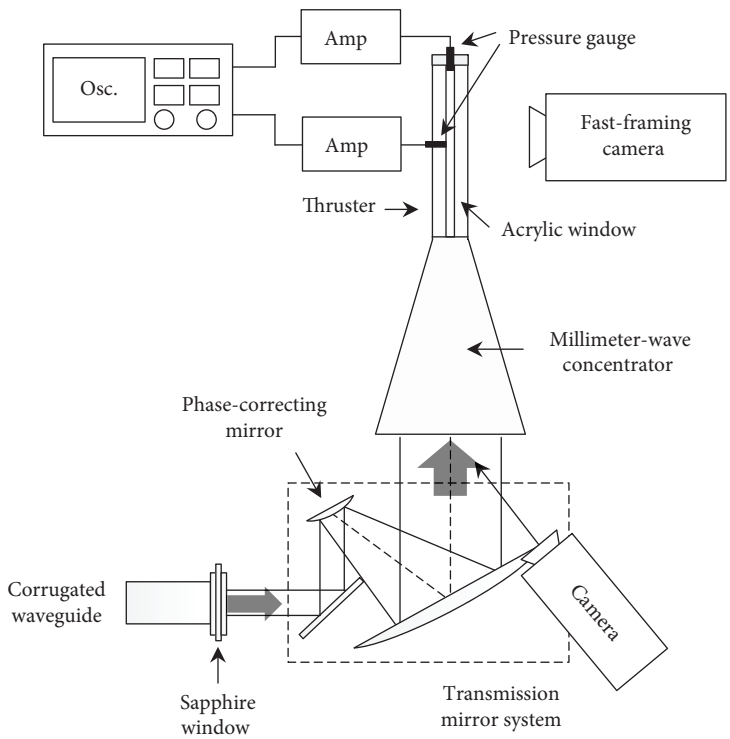

Figure 5: Setup for a launch experiment with long beam transmission using a concentrator [28].

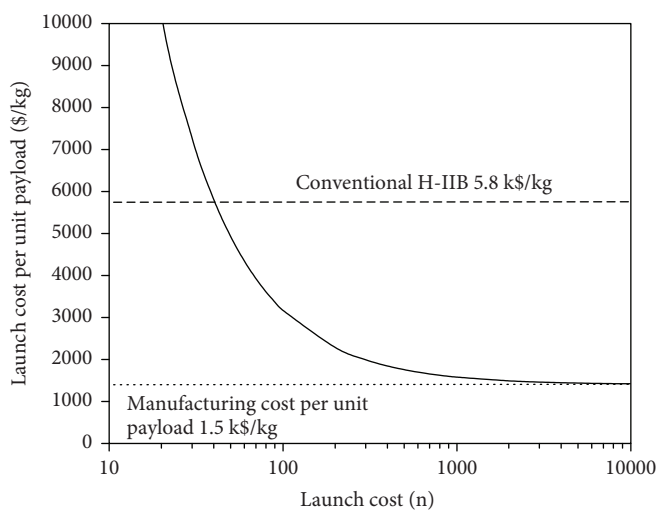

Figure 6: Estimated launch cost to LEO per unit payload as a function of launch counts. Dashed line: cost for H-IIB heavy; dotted line: manufacturing cost for *Microwave Rocket* and H-IIB second stage [14].

accounts for the major part of the new launch system. Although this initial cost could be as much as 3350 M$ including an energy storage facility, it will be amortized with launch counts and the cost per launch is decreased to the same level of conventional launch cost with about 42 launches, and finally 77% cost reduction is expected as shown in Figure 6 [14].

4.2. Small Payload Launch System Combining Microwave Rocket and NASA Microwave Thermal Thruster. Another feasibility study introduces a combination of *Microwave Rocket* as the first stage and a microwave thermal rocket studied by NASA as the second stage aiming at small payload launch to low earth orbit. The original NASA concept was to launch a vehicle by an unmanned aerial vehicle (UAV), and then initiate the microwave thermal rocket composed of a heat exchanger and a hydrogen propellant tank [10]. Replacement of the UAV by *Microwave Rocket* enables the second stage to start at high altitude with large initial velocity, resulting in low tank weight and low overall cost. Launch cost

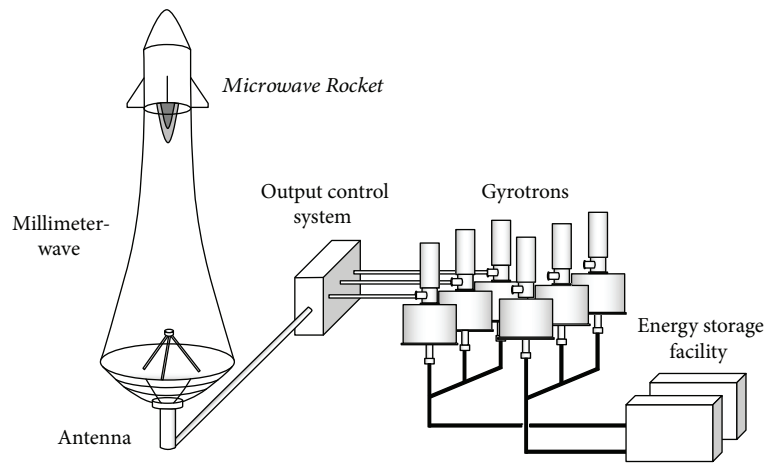

Figure 7: System Configuration of a beam facility.

per unit payload mass will be 5.8 k$/kg which is one-fourth of the UAV-assisted launch. The beam facility cost for launching an 8 kg satellite is estimated: the necessary output power is about 100 MW, and the gyrotrons and power supply cost 22 M$, while a transmitter antenna of 180 m in diameter costs 466 M$ [15].

4.3. Beam Facility Configuration on the Ground and Required Technologies in the Future. The beam facility consists of gyrotrons and a transmitter antenna. If a phased array antenna system is employed for beamforming to reduce the output power, an output power control system for synthesizing and dividing with phase controlling is required. The beam facility configuration is depicted in Figure 7.

In the ITER project, 24 gyrotrons are combined to have 20 MW heating in total [18]. There will be several restrictions like adjacent distance between gyrotrons, for instance, to avoid the interference of leakage magnetic field from superconducting magnets [29]. The gyrotron operation time of one launch is about 200 seconds. Even if ten launches are carried out every day, total operation time is only 200 hours per year, which is much shorter than expected lifetime of typical gyrotron system 5000 hours [5]. Flywheels utilized in nuclear fusion [30] and more advanced system, superconducting magnetic energy storage (SMES) system, are the candidates for an energy storage facility.

A phased array system which needs to control output power, frequency, and phase will make the required output power even smaller [31]. It will be effective to utilize a phase-locking technology to stabilize gyrotron's frequency and phase by inserting external signals to gyrotrons [32]. When a phased array system is not employed, a huge parabolic antenna will be used as an antenna. An antenna whose diameter is 50 m ~ 100 m can be constructed by hundreds of millions of dollars. The stratospheric platform airship program conducted by JAXA intended to transmit 1 MW electric power to the airship, using a parabolic antenna [33]. An optimal beam frequency has to be chosen by taking into account the resulting size of an antenna and a launch vehicle and the atmospheric attenuation of a beam. When a beam is transmitted by a Gaussian profile, the transmission distance theoretically determines the spread of the beam diameter. Although the directivity of a Gaussian beam is improved with a larger frequency, the atmospheric attenuation rate increases. Applied frequency will be chosen from the transmission windows in the range of 100 GHz calculated by a line by line method [6]. For *Microwave Rocket* launches in the future, it is necessary to amend the current Radio law which restricts the use of electromagnetic wave.

5. Propagation of Ionization Front and Filamentary Plasma Structure in Millimeter-Wave Discharge

Experimental studies of atmospheric microwave discharge have been conducted since the 1940s. However, studies using a millimeter-wave band have begun because of the widening use of gyrotrons. According to past studies, the propagation velocity of an ionization front in a millimeter-wave discharge is revealed to have a very different tendency from that in laser discharge, as presented in Figure 8, where the measured propagation velocities in a millimeter-wave discharge using a 170 GHz (wavelength, $\lambda = 1.76$ mm) gyrotron [34, 35] and a 110 GHz ($\lambda = 2.73$ mm) gyrotron [36] are shown along with those in laser discharge obtained using a CO_2 laser ($\lambda = 10.6\ \mu$m) with sufficiently large beam spot size [37–39]. The propagation velocity of an ionization front in a millimeter-wave discharge is greater than those in laser discharge by one order of magnitude.

In addition to its high propagation velocity, a millimeter-wave discharge plasma is known to have unique and fine structures as depicted in Figure 9. The plasma structure observed by Oda et al. [34, 35] in a 170 GHz, 1.5 GW/m^2 millimeter-wave beam is depicted in Figure 9(a). The branching structure is referred to as a comb-shaped structure. The structure called a fishbone shape is depicted in Figure 9(b). It was observed by Vikharev et al. [40] in a 35 GHz, 0.14 GW/m^2 millimeter-wave beam in helium gas at reduced pressure.

The microstructure called a quarter-wavelength structure was observed by Hidaka et al. [41] in a focused 110 GHz,

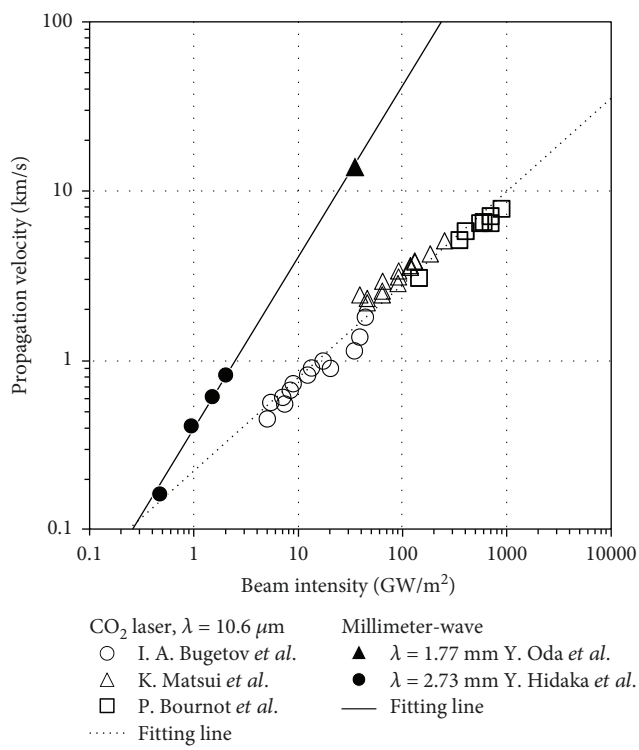

Figure 8: Ionization-front propagation velocity in an atmospheric millimeter-wave discharge [34, 36] and laser discharge [37–39].

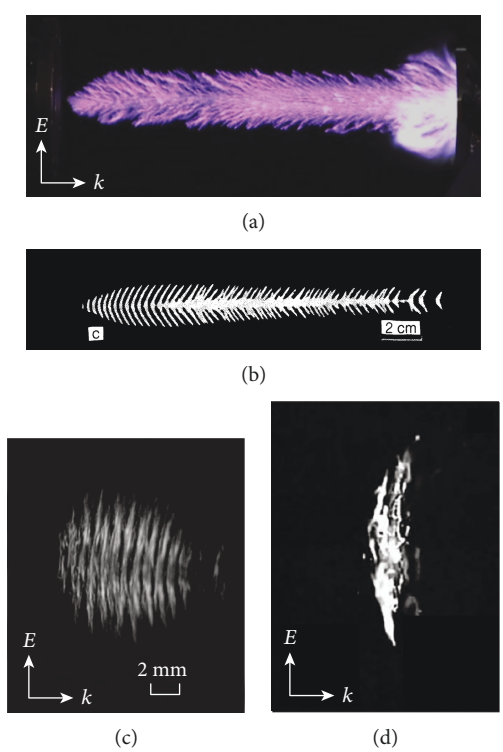

Figure 9: Filamentary plasma structures observed in experiments: (a) 170 GHz, 1.5 GW/m^2 [34, 35]; (b) 35 GHz, 0.14 GW/m^2 [40]; (c) 110 GHz, 35 GW/m^2, 0.8 atm [41]; (d) 28 GHz, 0.59 GW/m^2, 1 atm. [44]. k and E, respectively, denote the wave number vector and the electric field vector of an incident beam.

35 GW/m^2 beam, as depicted in Figure 9(c). Cook et al. also observed the filamentary structure in a 110 GHz millimeter-wave [42]. In this structure, the interval between neighboring filamentary plasmas extending in the electric field direction was about a quarter-λ.

In atmospheric discharges in a microwave beam, a streamer-like structure was observed at subcritical conditions and numerically reproduced by Khodataev [43]. It was found that breakdown occurred in an intense electric field near the surface of a thin plasma filament. A similar structure was obtained in a 28 GHz millimeter-wave beam as shown in Figure 9(d) [44].

Atmospheric millimeter-wave discharge physics remains unclear. Especially, the propagation mechanism of a millimeter-wave discharge at a beam intensity far below the breakdown threshold is under investigation.

6. Numerical Simulation of Millimeter-Wave Discharge Plasma

Numerical simulations are effective to clarify the formation mechanisms of these distinctive structures and in the end for an optimal thruster designing. Many researchers have been working on simulations. Millimeter-wave discharges are classifiable into two conditions, subcritical or undercritical, in which electric field intensities of the incident beam are, respectively, close to or far below the breakdown threshold.

The quarter-λ structure was obtained when the irradiated millimeter-wave is at the subcritical intensity. Boeuf et al. [45] reproduced this quarter-λ structure in an E-k plane. They coupled Maxwell's equations with an electron diffusion equation with effective diffusion coefficients and ionization frequencies computed using Bolsig+. Because of the reflection of incident waves on the plasma, an antinode of a standing wave was generated at quarter-λ ahead of the plasma resulting in the quarter-λ plasma structure as observed.

The comb-shaped filamentary structure was formed at much lower intensity than the breakdown threshold. Takahashi et al. [46, 47] proposed a numerical model considering compressibility of the ambient gas. Results showed that expansion behind a precursor shock wave enhances the effective field intensity to near the threshold in front of the plasma.

For cases in which shock expansion is not expected, we assumed hypothetical ionization frequencies higher than those obtained using Bolsig+. We reproduced a comb-shape filamentary plasma structure [48]. Figure 10 portrays the numerically computed plasma structure along with the experimentally observed structure, in both of which plasmoid pitch was approximately 0.9 λ. This structure is created by the wave reflections on the discrete plasmoid. The pitch was invariable for plasma density, millimeter-wave wavelength, and electric field intensity. The quarter-λ microstructure is apparent in each plasmoid when the ionization frequency was high and the diffusion coefficient was low.

Millimeter-wave discharge occurs even at the beam intensity far below breakdown threshold [44]. This discharge cannot be explained by field concentration nor by ambient gas expansion behind a blast wave [45, 46] and requires other

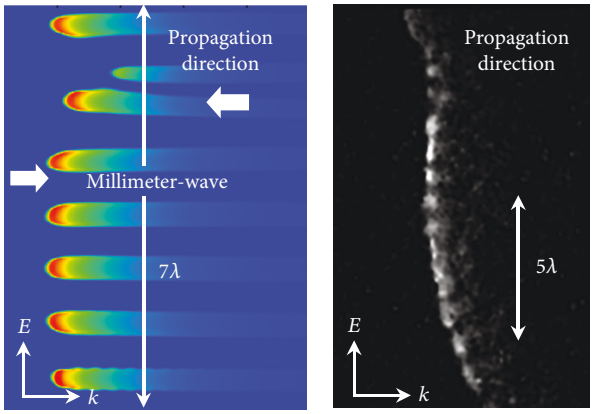

(a) (b)

Figure 10: Filamentary plasma structures in an atmospheric millimeter-wave discharge at the undercritical intensity: (a) computed density profile and (b) observed luminosity profile. 170 GHz; 1 GW/m^2 [48].

discharge sustention mechanisms. To derive the ionization frequencies at the undercritical intensity theoretically, an ionization model considering neutral gas excitation must be examined in the future work.

7. Summary

Microwave Rocket, one of beamed energy propulsion systems, is under development. Millimeter-wave-supported detonation driven by an atmospheric millimeter-wave discharge generates high pressures in a thruster tube, imparting impulsive thrust on a thrust wall. The repetitively pulsed detonation engine cycle produces continuous thrust. A thruster model of 126 g weight was launched to 1.2 m altitude using a QST gyrotron.

Flight analyses showed that *Microwave Rocket* can replace conventional chemical rockets with a significant improvement in a payload ratio and bring a drastic launch cost reduction. By utilizing *Microwave Rocket* as the first stage of the H-IIB heavy, the total mass of the vehicle is expected to be one-fifth of the conventional one which can directly improve the payload ratio by five times. The manufacturing cost of the gyrotrons is the substantial part of the *Microwave Rocket*, which can be recovered through 2000 launches, and as a result, the launch cost can be 77% lower than the conventional launch cost. Regarding the beam facility on the ground, conventional technologies utilized in the field of nuclear fusion researches can be used.

The physics of an atmospheric millimeter-wave discharge, especially the propagation velocity of the plasma front, is of interest as the thrust performance is directly related to it. The propagation velocity of the ionization front is much higher than those in laser discharge when shown as a function of beam intensity. However, the discharge at a beam intensity far below the breakdown threshold remains unclarified. A new ionization model would be an indispensable tool for it.

Conflicts of Interest

The authors declare that they have no conflicts of interest.

Acknowledgments

This work was presented at the 1st Asia-Pacific Conference on Plasma Physics, 18–23 September 2017, Chengdu, China, and was supported by JSPS KAKENHI Grant number JP15H05770.

References

[1] C. Phipps, M. Birkan, W. Bohn et al., "Review: laser-ablation propulsion," *Journal of Propulsion and Power*, vol. 26, no. 4, pp. 609–637, 2010.

[2] G. W. Jull, *Summary Report on SHARP (Stationary High-Altitude Relay Platform) Part A-Technical Feasibility of Microwave-Powered Airplanes*, CRC Report No. 1393, Communications Research Centre, Ottawa, 1985.

[3] K. Shimamura, H. Sawahara, A. Oda et al., "Feasibility study of microwave wireless powered flight for micro air vehicles," *Wireless Power Transfer*, vol. 4, no. 2, pp. 146–159, 2017.

[4] K. Komurasaki and B. Wang, "Laser propulsion," in *Encyclopedia of Aerospace Engineering*, R. Blockley and W. Shyy, Eds., pp. 1351–1360, John Wiley & Sons Ltd., Chichester, UK, 2010.

[5] P. George and R. Beach, "Beamed-energy propulsion (BEP) study," US Patent NASA/TM-2012-217014, 2012.

[6] K. Komurasaki, K. Shimamura, and M. Fukunari, "Microwave rocket "propelled by millimeter wave"," *Journal of Plasma and Fusion Research*, vol. 93, no. 10, pp. 465–490, 2017, (In Japanese).

[7] M. Fukunari, K. Komurasaki, Y. Nakamura, Y. Oda, and K. Sakamoto, "Rocket propulsion powered using a gyrotron," *Journal of Energy and Power Engineering*, vol. 11, no. 6, pp. 363–371, 2017.

[8] A. Kantrowitz, "Propulsion to orbit by ground-based laser," *Astronautics and Aeronautics*, vol. 10, pp. 74–76, 1972.

[9] L. Myrabo, "World record flights of beam-riding rocket lightcraft - demonstration of "disruptive" propulsion technology," in *37th Joint Propulsion Conference and Exhibit, Joint Propulsion Conferences*, Salt Lake City, UT, USA, July 2001.

[10] K. L. Parkin and D. D. Murakami, "An overview of the NASA Ames Millimeter-Wave Thermal Launch System," in *48th AIAA/ASME/SAE/ASEE Joint Propulsion Conference & Exhibit*, Atlanta, GA, USA, July-August 2012.

[11] H. Katsurayama, K. Komurasaki, and Y. Arakawa, "A preliminary study of pulse-laser powered orbital launcher," *Acta Astronautica*, vol. 65, no. 7-8, pp. 1032–1041, 2009.

[12] T. J. Kare, "Modular laser options for HX laser launch," in *Proceeding of 3rd International Symposium on Beamed Energy Propulsion, AIP Conference Proceedings*, pp. 128–139, Troy, NY, USA, October 2005.

[13] E. W. Davis and F. B. Mead Jr., "Review of laser lightcraft propulsion system," in *Proceeding of 3rd International Symposium on Beamed Energy Propulsion, AIP Conference Proceedings*, pp. 283–294, Kailua-Kona, Hawaii, November 2008.

[14] M. Fukunari, A. Arnault, T. Yamaguchi, and K. Komurasaki, "Replacement of chemical rocket launchers by beamed energy propulsion," *Applied Optics*, vol. 53, no. 31, pp. I16–I22, 2014.

[15] K. Kakinuma, M. Fukunari, T. Yamaguchi et al., "Two-stage-to-orbit transporting system combining microwave rocket and microwave thermal rocket for small satellite launch," *Transactions of the Japan Society for Aeronautical and Space Sciences, Aerospace Technology Japan*, vol. 14, no. 30, pp. Pb_99–Pb_103, 2016.

[16] K. Sakamoto, A. Kasugai, K. Takahashi, R. Minami, N. Kobayashi, and K. Kajiwara, "Achievement of robust high-efficiency 1 MW oscillation in the hard-self-excitation region by a 170 GHz continuous-wave gyrotron," *Nature Physics*, vol. 3, no. 6, pp. 411–414, 2007.

[17] T. Kariya, T. Imai, R. Minami et al., "Development of gyrotrons for fusion with power exceeding 1 MW over a wide frequency range," *Nuclear Fusion*, vol. 55, no. 9, article 093009, 2015.

[18] M. A. Henderson and G. Saibene, "Critical interface issues associated with the ITER EC system," *Nuclear Fusion*, vol. 48, no. 5, article 054017, 2008.

[19] T. Endo, J. Kasahara, A. Matsuo, S. Sato, K. Inaba, and T. Fujiwara, "Pressure history at the thrust wall of a simplified pulse detonation engine," *AIAA Journal*, vol. 42, no. 9, pp. 1921–1930, 2004.

[20] T. Nakagawa, Y. Mihara, K. Komurasaki, K. Takahashi, K. Sakamoto, and T. Imai, "Propulsive impulse measurement of a microwave-boosted vehicle in the atmosphere," *Journal of Spacecraft and Rockets*, vol. 41, no. 1, pp. 151–153, 2004.

[21] B. Wang, K. Michigami, K. Komurasaki, and Y. Arakawa, "Thrust measurement for laser-detonation propulsion with a solid-state laser," *Journal of Propulsion and Power*, vol. 29, no. 1, pp. 276–278, 2013.

[22] Y. Oda, T. Shibata, K. Komurasaki, K. Takahashi, A. Kasugai, and K. Sakamoto, "Thrust performance of microwave rocket under repetitive-pulse operation," *Journal of Propulsion and Power*, vol. 25, no. 1, pp. 118–122, 2009.

[23] R. Komatsu, T. Yamaguchi, Y. Oda et al., "Thrust augmentation of microwave rocket with high-power and high-duty-cycle operation," *Journal of the Japan Society for Aeronautical and Space Sciences*, vol. 60, no. 6, pp. 235–237, 2012.

[24] M. Fukunari, T. Yamaguchi, K. Komurasaki et al., "Air-breathing system using reed valve for pulse detonation microwave rocket," *Transactions of the Japan Society for Aeronautical and Space Sciences, Aerospace Technology Japan*, vol. 14, pp. 1–7, 2016.

[25] M. Fukunari, R. Komatsu, A. Arnault, T. Yamaguchi, K. Komurasaki, and Y. Arakawa, "Air-breathing performance of microwave rocket with reed valve system," *Vacuum*, vol. 88, pp. 155–159, 2013.

[26] K. Tabata, F. Nguyen, Y. Harada et al., "Numerical calculation on air-inlet design of microwave rocket," *Journal of the Japan Society for Aeronautical and Space Sciences*, vol. 66, no. 5, pp. 128–134, 2018.

[27] M. Fukunari, N. Wongsuryrat, T. Yamaguchi, Y. Nakamura, K. Komurasaki, and H. Koizumi, "Design of a millimeter-wave concentrator for beam reception in high-power wireless power transfer," *Journal of Infrared, Millimeter, and Terahertz Waves*, vol. 38, no. 2, pp. 176–190, 2017.

[28] M. Fukunari, T. Yamaguchi, Y. Nakamura et al., "Thrust generation experiments on microwave rocket with a beam concentrator for long distance wireless power feeding," *Acta Astronautica*, vol. 145, pp. 263–267, 2018.

[29] K. Kajiwara, Y. Oda, A. Kasugai et al., "Effect of the stray magnetic field on the gyrotrons for ITER," in *2009 34th International Conference on Infrared, Millimeter, and Terahertz Waves*, Busan, South Korea, September 2009.

[30] R. Shimada, "Power conversion and energy storage system for a fusion reactor 3. Performance of large electric power equipment and future view 3.3 kinetic energy storage (flywheel, compressed air energy storage)," *Journal of Plasma and Fusion Research*, vol. 80, no. 7, pp. 572–577, 2004.

[31] K. Kakinuma, F. Nguyen, M. Fukunari, K. Komurasaki, and H. Koizumi, "Application of active phased array antenna for millimeter-wave transfer to beamed energy launch vehicles," *Space Solar Power Systems*, vol. 3, pp. 30–37, 2018.

[32] G. G. Denisov and A. G. Litvak, "New results of development of gyrotrons for plasma fusion installations," in *26th IAEA Fusion Energy Conference*, Kyoto, Japan, 2016.

[33] T. Fujihara and K. Eguchi, "Research and development on regenerative fuel cells for stratospheric platform airship: ground-based testing of 1 KW RFC system models," JAXA Tech. Rep. JAXA-RM-07-014, 2008, (In Japanese).

[34] Y. Oda, K. Komurasaki, and K. Sakamoto, "Dynamics and structure of ignition process in plasmas," *Journal of Plasma and Fusion Research*, vol. 84, no. 6, pp. 343–347, 2008.

[35] Y. Oda, K. Komurasaki, K. Takahashi, A. Kasugai, and K. Sakamoto, "Plasma generation using high-power millimeter-wave beam and its application for thrust generation," *Journal of Applied Physics*, vol. 100, no. 11, article 113307, 2006.

[36] Y. Hidaka, E. M. Choi, I. Mastovsky et al., "Plasma structures observed in gas breakdown using a 1.5 MW, 110 GHz pulsed gyrotron," *Physics of Plasmas*, vol. 16, no. 5, article 055702, 2009.

[37] I. A. Bufetov, A. M. Prokhorov, V. B. Fedorov, and V. K. Fomin, "Optical discharge accompanying a restriction imposed on lateral expansion of gas and a reduction in the threshold of light-induced detonation," *JETP Letters*, vol. 39, pp. 258–261, 1987.

[38] K. Matsui, T. Shimano, J. A. Ofosu, K. Komurasaki, T. Schoenherr, and H. Koizumi, "Accurate propagation velocity measurement of laser supported detonation waves," *Vacuum*, vol. 136, pp. 171–176, 2017.

[39] P. Bournot, P. A. Pincosy, G. Inglesakis, M. Autric, D. Dufresne, and J. P. Caressa, "Propagation of a laser-supported detonation wave," *Acta Astronautica*, vol. 6, no. 3-4, pp. 257–267, 1979.

[40] A. L. Vikharev, V. B. Gil'denburg, S. V. Golubev et al., "Nonlinear dynamics of a freely localized microwave discharge in an electromagnetic wave beam," *Soviet Physics - Journal of Experimental and Theoretical Physics*, vol. 67, no. 4, pp. 724–728, 1988.

[41] Y. Hidaka, E. M. Choi, I. Mastovsky, M. A. Shapiro, J. R. Sirigiri, and R. J. Temkin, "Observation of large arrays of plasma filaments in air breakdown by 1.5-MW 110-GHz gyrotron pulses," *Physical Review Letters*, vol. 100, no. 3, article 035003, 2008.

[42] A. M. Cook, J. S. Hummelt, M. A. Shapiro, and R. J. Temkin, "Observation of plasma array dynamics in 110 GHz millimeter-wave air breakdown," *Physics of Plasmas*, vol. 18, no. 10, article 100704, 2011.

[43] K. V. Khodataev, "Microwave discharges and possible applications in aerospace technologies," *Journal of Propulsion and Power*, vol. 24, no. 5, pp. 962–972, 2008.

[44] Y. Harada, Y. Nakamura, K. Komurasaki et al., "Structural change of plasma at various ambient pressures in 28 GHz millimeter-wave discharges," *Frontier of Applied Plasma Technology*, vol. 10, p. 1, 2017.

[45] J.-P. Boeuf, B. Chaudhury, and G. Q. Zhu, "Theory and modeling of self-organization and propagation of filamentary plasma arrays in microwave breakdown at atmospheric pressure," *Physical Review Letters*, vol. 104, no. 1, article 015002, 2010.

[46] M. Takahashi, Y. Kageyama, and N. Ohnishi, "Joule-heating-supported plasma filamentation and branching during subcritical microwave irradiation," *AIP Advances*, vol. 7, no. 5, article 055206, 2017.

[47] M. Takahashi and K. Komurasaki, "Discharge from a high-intensity millimeter wave beam and its application to propulsion," *Advances in Physics: X*, vol. 3, no. 1, pp. 113–144, 2018.

[48] Y. Nakamura, K. Komurasaki, M. Fukunari, and H. Koizumi, "Numerical analysis of plasma structure observed in atmospheric millimeter-wave discharge at under-critical intensity," *Journal of Applied Physics*, vol. 124, no. 3, article 033303, 2018.